Official Journal Issued by Faculty of Veterinary Medicine

Benha Veterinary Medical Journal

Journal homepage: https://bvmj.journals.ekb.eg/

Since 1990

Original Paper

Antidiabetic, renoprotective, and cardioprotective effects of coriander seed and garlic extracts in experimentally induced diabetes

Rania Mohamed Elbatawy, Abdel-Baset I. El-Mashad, Ahmed A. Tantawy, Shawky A. Mostafa, Aziza A. Amin

.Department of Pathology, Faculty of Veterinary Medicine, Benha University, Toukh 13736, Egypt

ARTICLE INFO

Keywords

STZ-induced diabetes

Coriander seed extract

Garlic extract

Histopathology

Immunohistochemistry

Received 06/07/2025
Accepted 08/08/2025
Available On-Line
xx/xx/2025

ABSTRACT

The study investigates the potential antidiabetic, renoprotective, and cardioprotective effects of coriander seed extract (CSE) and garlic extract (GE) in streptozotocin (STZ)-induced diabetic rats. Thirty adult male rats were divided into five groups: a control group, a diabetic untreated group, and diabetic groups treated with glibenclamide, CSE and GE. Treatment continued daily for 28 days. Serum biochemical studies showed that diabetic rats had significantly higher levels of glucose, creatinine, urea, uric acid, Creatine Kinase-MB (CK-MB) and Lactic Dehydrogenase (LDH) levels than the control group. Histopathological and immunohistochemical examinations revealed marked hypocellularity, degeneration, and necrosis of pancreatic islets, accompanied by a significant reduction in insulin expression in comparison with the control. Additionally, diabetic rats exhibited structural damage in the kidneys and heart, characterized by tubular epithelial degeneration and necrosis and myocardial myomalacia. Administration of CSE and GE significantly mitigated these biochemical and histological changes, with CSE demonstrating superior protective effects. These results highlight the therapeutic potential of CSE and GE particularly emphasizing CSE as an effective natural therapy for managing diabetes and its associated renal and cardiac complications.

1. INTRODUCTION

Diabetes is a chronic metabolic disorder characterized by elevated blood glucose levels, insulin resistance, or impaired insulin secretion affecting various animal species. (Nambirajan et al., 2018). According to recent estimates from the World Health Organization, diabetes prevalence continues to rise globally, significantly increasing morbidity and mortality related to diabetic complications (Wild et al., 2004). Diabetes is primarily categorized into immune-mediated diabetes (Type 1 diabetes) and insulin resistance diabetes (Type 2 diabetes) (Saunders et al., 2022). Experimental induction of diabetes commonly utilizes agents such as Alloxan or streptozotocin (STZ), which specifically induce oxidative stress leading to selective necrosis and apoptosis of pancreatic β-cells, thereby causing diabetes mellitus (Ahmed et al., 2023). Chronic hyperglycemia associated with diabetes triggers numerous pathophysiological changes, notably Microvascular damage which significantly affects cell metabolism, and lead to progressive lesions in several organs, such as kidneys, eyes, nerves, liver, and blood vessels (Babel and Dandekar, 2021). Diabetic nephropathy (DN), also termed diabetic kidney disease (DKD), is a serious complication of diabetes, affecting approximately 25% of individuals diagnosed with diabetes (Thijs et al., 2021). Typically, the progression of DN is marked by the onset of microalbuminuria progressing to macroalbuminuria (Tong et al., 2020). The histopathological renal changes associated with DN are largely attributed to excessive generation of reactive oxygen species (ROS) and reactive nitrogen species (RNS) mediated by chronic hyperglycemia (Wang and Zhang, 2024), resulting in oxidative stress, lipid peroxidation, protein denaturation, and mitochondrial DNA damage (Rashid et al., 2023).

Similarly, diabetic cardiomyopathy (DiaCM), characterized by ventricular dysfunction independent of atherosclerosis or hypertension (Shabab et al., 2024). Oxidative stress resulting from increased ROS and RNS generation is central to cardiac inflammation and structural remodeling observed in DiaCM(Tan et al., 2020).

Currently, clinical management strategies for diabetes primarily involve insulin therapy and oral hypoglycemic drugs; however, these treatments often pose risks of adverse side effects and limited efficacy in halting disease progression (Aloke et al., 2022). Consequently, identifying therapeutic compounds derived from natural sources with fewer adverse effects has emerged as a significant research focus. Medicinal plants and herbs represent a significant resource, offering multiple bioactive compounds that have demonstrated efficacy in managing chronic metabolic diseases, including diabetes (Sadeghabadi et al., 2022).

Garlic (*Allium sativum*) is commonly used as a flavoring agent and functional food as well as traditional medicine, with a wide range of biological effects, such as anticancer, antioxidant, antimicrobial, anti-mutagenic, anti-asthmatic, and immunomodulatory activities (Okoro et al., 2023). The characteristic protective effects of garlic are primarily attributed to the presence of sulfur and a variety of compounds, such as allicin, alliin, and methyl allyl-trisulfide (Song et al., 2015). Previous studies have documented that garlic is an effective herbal plant for controlling blood glucose levels (Lidiková et al., 2022). Additionally, garlic could also be effective in reducing hyperglycemic

* Correspondence to: Rania.Elbatawy@fvtm.bu.edu.eg

complications due to its antioxidant effect by scavenging ROS (Padiya et al., 2011)

Coriander (*Coriandrum sativum L.*) is identified as one of the oldest medicinal herb, contains multiple bioactive components such as flavonoids (quercetin and isoquercitrin, rutin), terpenes (linalool), terpenoids, polyphenols, fatty acids, coumarins and vitamins which could be responsible for its therapeutic action (Sobhani et al., 2022). Furthermore, *coriander sativum* demonstrated antioxidant, antidiabetic, anticonvulsant, anti-inflammatory, antimutagenic, antibacterial activity among others, in addition to hormone balancing and analgesic characteristics (Priya and Kumar, 2021).

Therefore, this study aimed to assess and compare the antidiabetic, renal, and cardiac protective effects of coriander seed extract (CSE) and garlic extract.

2.MATERIAL AND METHODS

Ethical approval

The Scientific Research Ethics Committee, Faculty of Veterinary Medicine, Benha University, approved all experimental procedures performed in this work (Ethical Approval number: BUFVTM 10-11-23).

Chemicals

Streptozotocin (STZ) was obtained from Sigma-Aldrich (USA). Glibenclamide (Daonil®) 5mg was purchased from Sanofi Specialized Pharmaceuticals Company, Cairo, Egypt. All other chemicals used in this study were bought from commercial suppliers as high-analytical grade.

Preparation of Plant Extracts

Coriander seed extract (CSE) and garlic extract (GE) were prepared according to the method described by Eidi et al., (2006). Prepared extracts were stored at -4°C until use.

Induction of diabetes mellitus

Streptozotocin (STZ) was dissolved in 0.1 M citrate buffer at pH 4.5. Diabetes was induced using a single intraperitoneal injection of STZ (50 mg/kg body weight). After 72 hours from injection, rats with fasting blood glucose higher than 250 mg/dl were considered diabetic (El-Shaer et al., 2023).

Experimental animals

Thirty adult male albino rats weighing 200 ± 20 g were obtained from the Experimental Animal House, Egyptian Company for Production of Serums, Vaccines, and Drugs, Helwan. Animals were housed in stainless-steel cages under controlled hygienic conditions. Prior to the experiment, rats were acclimated for one week at ambient temperature of 23 ± 3 °C, a natural 12-hour dark/light cycle, and free access to clean water and a balanced commercial diet.

Experimental design

The rats were randomly divided into five equal groups (n=6 each):

Group 1 (control): Received citrate buffer orally (0.5 ml/kg).

Groups 2-5: Diabetes induced by intraperitoneal injection of STZ (50 mg/kg body weight).

Group 2: Diabetic untreated.

Group 3: Diabetic rats treated orally with glibenclamide (0.5 mg/kg bw) (Rabbani et al., 2010).

Group 4: Diabetic rats treated orally with CSE (250 mg/kg bw) (Naquvi et al., 2004).

Group 5: Diabetic rats treated orally with GE (250 mg/kg bw) (Mittal and Juyal, 2012, Kaur et al., 2016).

Treatments were administered daily for 28 consecutive days after induction of diabetes (Soni et al., 2009).

Serum biochemical analysis

At the end of the experimental period, blood samples were collected from the orbital sinus of each rat in sodium fluoride tubes for serum glucose determination and gel activator tubes for renal and cardiac function biomarker evaluations. Blood was centrifuged at 3,000 rpm for 15 min for serum separation and stored at -20 °C until used. Serum glucose, creatinine, urea, uric acid, CK-MB and LDH were measured using commercial reagent kits from Spectrum Company, Egypt according to Tiffany et al., (1972), Young, (1995), Dunn et al., (2004), Ghanbari et al., (2016) and Jing et al., (2018) respectively.

Histopathological study

Small tissue specimens were collected from the pancreas, kidneys, and heart of rats from all groups and immediately fixed in 10% neutral buffered formalin. Fixed tissues were dehydrated, cleared, and embedded in paraffin wax. Five µm-thick paraffin sections were routinely prepared and stained with hematoxylin and eosin (H&E) stain (Bancroft and Layton 2019), as well as Periodic Acid-Schiff (PAS) for kidney sections to examine renal tubular brush borders, glomerular and basement membranes (Layton and Bancroft, 2019).

Immunohistochemical Examination

Immunohistochemical detection of insulin was conducted on pancreatic tissue sections. The, Deparaffinized and rehydrated sections were incubated with a polyclonal guinea pig anti-insulin antibody (N1542, Dako, Carpinteria, CA, USA 1:100 dilution) using avidin-biotin-peroxidase technique (Abunasef et al., 2014). Both histopathological and immunohistochemical sections were examined and photographed using a Nikon Eclipse E800 microscope equipped with a digital camera.

Assessment of Histopathological damage

The following semi-quantitative scoring system based on severity, distribution and type of lesion is used, typically on a 0-4 scale:

Score	Severity	Description
0	Normal	No visible lesion
1	Minimal	<10% of the section affected, very mild alterations
2	Mild	10-25% affected, mild structural changes
3	Moderate	25-50% affected, obvious tissue damage
4	Severe	>50% affected, extensive tissue destruction

The total score is then calculated by summing the individual scores, to get an overall tissue damage index: 0–3 = Normal or minimal injury; 4–7 = Mild injury; 8–12 = Moderate injury; >12 = Severe injury. The grading system was conducted on five H&E sections of pancrease, kidney and heart as well as insulin immunoreactivity from each group (Chavez et al., 2016) with modification.

Statistical analysis:

Data from biochemical assays and histopathological lesions were analyzed using GraphPad Prism software version 9. Following a one-way ANOVA, Tukey's multiple comparisons test was employed. Results were expressed as mean ± standard deviations (SD). Statistical significance was set at $p < 0.05$.

3. RESULTS

Serum biochemical findings

Serum glucose, creatinine, urea, uric acid, CK-MB, and LDH levels were significantly elevated ($p<0.0001$) in STZ diabetic rats compared to the control group (Fig.1). Treatment with glibenclamide, CSE and GE resulted in significant reductions ($p<0.001$) in these serum biomarkers compared to STZ group. CK-MB and LDH levels showed significant improvement ($p<0.001$) with CSE and GE treatments compared to glibenclamide-treated group, approaching levels similar to the control.

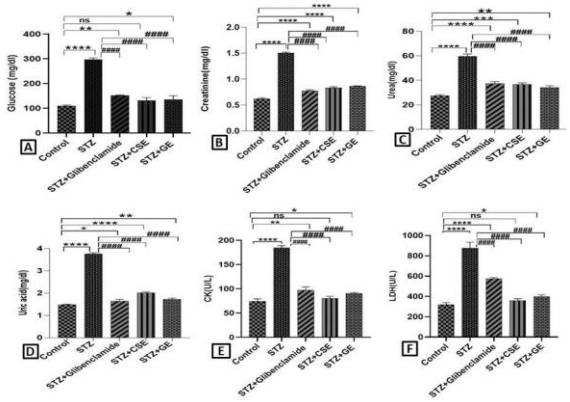

Fig.1 Effect of STZ, glibenclamide, CSE and GE on serum glucose (A), creatinine (B), urea (C), uric acid (D), CK (E), and LDH (F) activities. Asterisks (*) denote significance vs. control: ****$p < 0.0001$, ***$p < 0.001$, **$p < 0.01$, *$p < 0.05$; Hashtags (#) denote significance vs. STZ group (####$p < 0.0001$); "ns" indicates non-significant differences. The data are expressed as mean ± SD.

Histopathological findings

Pancreas:

The examined pancreatic sections from a control group revealed normal pancreatic architecture. The islets of Langerhans showed typical size, and shape, well-demarcated rounded structures, embedded within the acinar tissue, and consisting of large spherical eosinophilic endocrine cells interspersed with capillaries (Fig.2A). The untreated STZ diabetic rats exhibited severe hypocellularity, degeneration, and necrosis of the islets of Langerhans (Fig. 2B), with occasional mononuclear inflammatory cells infiltration (Fig. 2C). Multifocally, there were dissociation, necrosis, and degeneration of the pancreatic acini. Additionally, the interlobular ducts were dilated and contained retained eosinophilic secretion. Diabetic rats treated with glibenclamide showed moderate improvement, with increased islet size and cell number (Fig. 2D). Notably, treatment with CSE resulted in significant improvement, characterized by reduced necrosis and increased islet size and cellularity (Fig. 2E) compared to glibenclamide; with occasional mild lymphocytic infiltration at the periphery of few islets of Langerhans. GE treatment also improved islet histology but to a lesser extent than CSE (Fig. 2F).

Immunohistochemical Findings

Immunohistochemical staining for insulin revealed positive immunoreactivity in the pancreatic islets, characterized by dense, brown-colored cytoplasmic staining of β cells. The pancreatic sections of control rats demonstrated strong, uniform staining of abundant insulin granules in β-cells (Fig.3A). On contrast, the diabetic group exhibited significantly reduced insulin immunoreactivity (Fig.3B) characterized by a diminished number of insulin-positive β-cells and weaker staining intensity (Fig.3C). Treatment with glibenclamide (Fig.3D), CSE (Fig.3E), and GE (Fig.3F) significantly enhanced insulin immunoreactivity, with CSE-treated rats showed the most substantial improvement in β-cell density and insulin expression, followed by GE and glibenclamide treatments.

Fig. 2: Histopathological alterations in pancreatic tissues stained with H&E

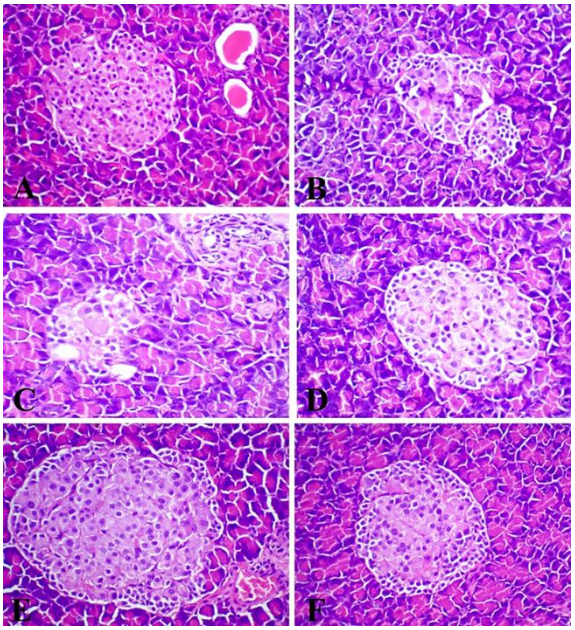

across experimental groups ×400. (A) Control group showing normal pancreatic architecture, with well-defined islets of Langerhans composed of eosinophilic endocrine cells and intact acinar tissue. (B-C) Diabetic untreated group revealing hypocellularity, degeneration and necrosis of islets cells with mononuclear inflammatory infiltrates. (D) Glibenclamide-treated group showing moderate restoration of islet morphology, with increased cellularity and mild necrosis of islets cells. (E) CSE-treated group revealing marked improvement in pancreatic pathology, characterized by increased islet size, reduced necrosis, and few lymphocytic infiltrations. (F) GE-treated group revealing partial amelioration of islet damage.

Fig. 3: Immunohistochemical staining for insulin in pancreatic tissues across

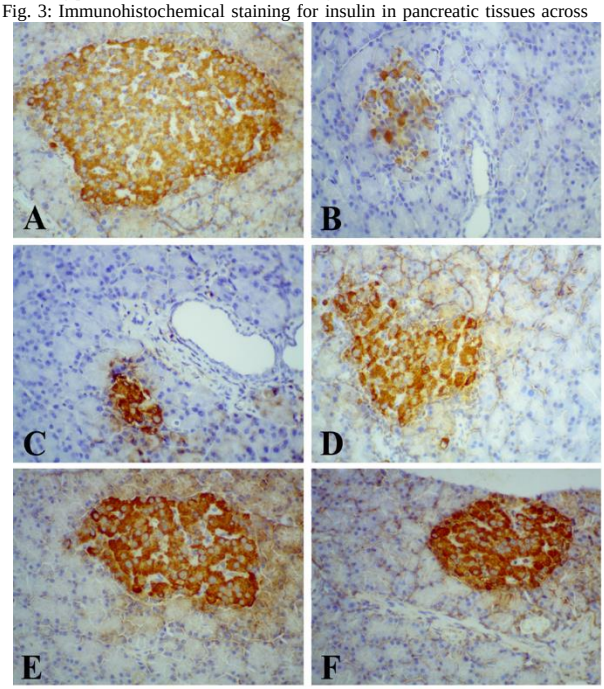

experimental groups ×400. (A) Control group showing intense, uniform cytoplasmic staining of β-cells. (B-C) STZ diabetic group revealing, marked reduced immunoreactivity, characterized by sparse insulin-positive β-cells and weak staining intensity. (D) Glibenclamide-treated group displaying moderate immunoreactivity of insulin-positive β-cells, staining comparable to control. (E) CSE-treated group demonstrating dense immunopositive reaction. (F) GE-treated groups showing moderate immunoreactivity.

Kidneys

The H&E-stained renal sections of the control group displayed normal histological architecture with intact glomeruli and renal convoluted tubules. Glomeruli showed normal histological criteria of the mesangium and glomerular capillaries and the proximal convoluted tubules in the cortex

were lined with simple cuboidal epithelium (Fig.4A). Contrary, the examined kidney sections of STZ diabetic rats revealed severe renal damage predominantly within cortical tubules. Prominent clear cell tubules with swollen, pale, vacuolated cytoplasm in the proximal and distal convoluted tubules were prevalent (Fig. 4B), Moreover, some renal sections showed apoptotic bodies inside the renal tubular lumens (Fig.4C), Multifocally, tubular epithelial cells of renal cortex showed coagulative necrosis characterized by indistinct cell borders, hypereosinophilic cytoplasm, and nuclear pyknosis (Fig.4D). Occasional necrotic areas revealed disruption of tubular architecture along with disorganization of peritubular capillaries, and replacement by edema admixed with cellular debries, hemorrhage, few macrophages and lymphocytes (Fig.4E). Less affected tubules were ectatic and occasionally contained proteinaceous eosinophilic casts or rare cellular debris (Fig.4F). Additionally, there were moderate congestion with perivascular edema and peritubular macrophages and lymphocytes aggregates and hemorrhages. Occasional vascular injuries characterized by endothelial cell proliferation, and vacuolation of the blood vessel wall were also observed

Kidneys from Glibenclamide-treated rats (Fig. 5A, B) partially maintained normal architecture with moderate epithelial degeneration or coagulative necrosis of convoluted tubules and occasional ectatic tubules with intraluminal casts. Furthermore, there was mild congestion, perivascular edema and vascular wall degeneration with interstitial mononuclear leukocytic cellular aggregates. Kidneys from CSE-treated rats (Fig.5C, D) largely maintained normal architecture, with only mild epithelial degeneration or coagulative necrosis in a few tubules and occasional hyaline casts in lumen of cortical tubules. Occasionally, there was mild congestion and perivascular edema, whereas the vascular damage was negligible. Similarly, kidneys from GE-treated rats (Fig. 5E, F) preserved renal structure in the majority of renal tubules with mild congestion of intertubular capillaries, degeneration or coagulative necrosis of tubular epithelial cells and intraluminal casts. Moreover, vacuolation of the vascular walls, perivascular edema, and peritubular leukocytic cellular infiltration were infrequently observed.

PAS-stained sections of control group revealed that basement membranes of Bowman's capsule, glomeruli and tubules were bright pink and of equal thickness. The cytoplasm of proximal epithelial cells was light pink and the apical brush borders are pink and easy to discern (Fig. 6A). The renal sections of STZ diabetic rats (Fig. 6B) exhibited cytoplasmic vacuoles with loss or fragmentation of the brush borders in the proximal convoluted tubules, with occasional prominent PAS-positive material accumulation in tubular lumenae. Occasionally, the basement membranes of glomerular capillaries and Bowman's capsules were mildly thickened by PAS-positive material (Fig. 6C). PAS-stained kidney sections of diabetic rats treated with glibenclamide partially retained normal PAS staining of glomeruli and tubules, with occasional loss or fragmentation of the brush borders of a few renal tubules and mild thickening of the glomerular tuft basement membranes (Fig. 6D). CSE-treated kidneys largely preserved normal PAS staining of glomeruli and tubules, with rare loss or fragmentation of the brush borders in the proximal epithelial cells (Fig. 6E). Similarly, diabetic rats treated with GE, revealed also normal PAS staining of the glomeruli and majority of convoluted tubules with occasional loss or fragmentation of the brush borders in few proximal tubules (Fig. 6F).

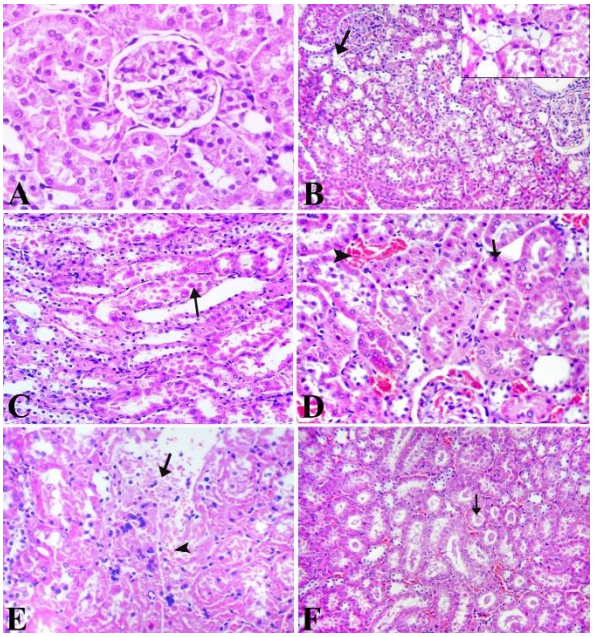

Fig 4: Representative photomicrographs of H&E stained-renal tissue of control and diabetic rats. (A) Control group displaying normal histological architecture with intact glomeruli and renal convoluted tubules. (B-F) Diabetic rats showing (B) marked clear cell tubules (arrow) characterized by swollen pale vacuolated cytoplasm (inset); (C) apoptotic bodies inside some renal tubular lumens (arrow); (D) coagulative necrosis of tubular epithelial cells (arrow) characterized by indistinct cell borders, hypereosinophilic cytoplasm, and nuclear pyknosis, note also congestion of the intertubular capillaries (arrowhead); (E) extensive necrotic area with disruption of tubular architecture (arrow) and its replacement by cellular debries, hemorrhage (arrowhead) few macrophages and lymphocytes; (F) numerous proteinaceous eosinophilic casts (arrow) in renal convoluted tubules. (B,C, F) ×200; (A,inset, D, E) ×400.

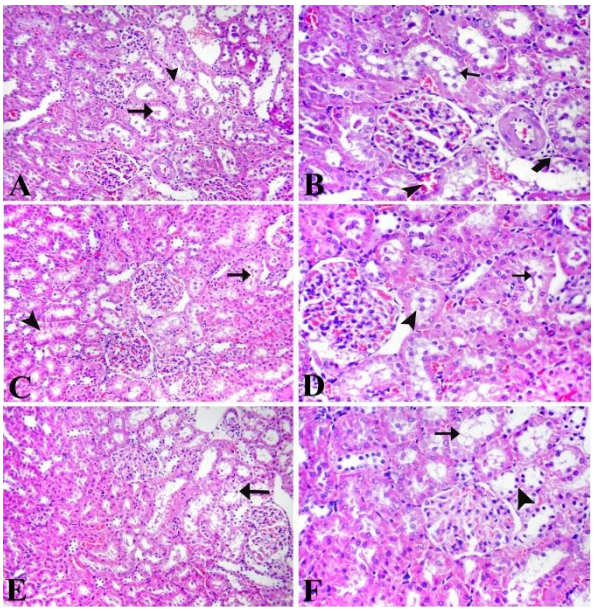

Fig.5 Representative photomicrographs of renal sections of diabetic rats treated with glibenclamide (A, B), CSE (C, D) and GE (E, F). (A-B) Glibenclamide group showing (A) moderate epithelial degeneration and coagulative necrosis of convoluted tubules (arrowhead) with intraluminal eosinophilic debris (arrow), (B) higher magnification exhibiting epithelial degeneration (thin arrow) and necrosis, note also mild congestion (arrowhead) and perivascular inflammatory edema (thick arrow). (C-D) CSE group revealing (C) largely preserved normal architecture with mild epithelial degeneration (arrowhead) and hyaline casts in a few tubules (arrow), (D) higher magnification showing mild epithelial degeneration (arrowhead) and hyaline casts in a few tubules (arrow). (E-F) GE group demonstrating (E) preserved renal architecture in the majority of tubules, with mild degeneration of tubular epithelial cells (arrow), (F) higher magnification showing mild epithelial degeneration. (arrow) and necrosis with pyknotic nuclei in a few tubules (arrowhead). (A, C, E) H&E ×200; (B, D, F) H&E ×400;

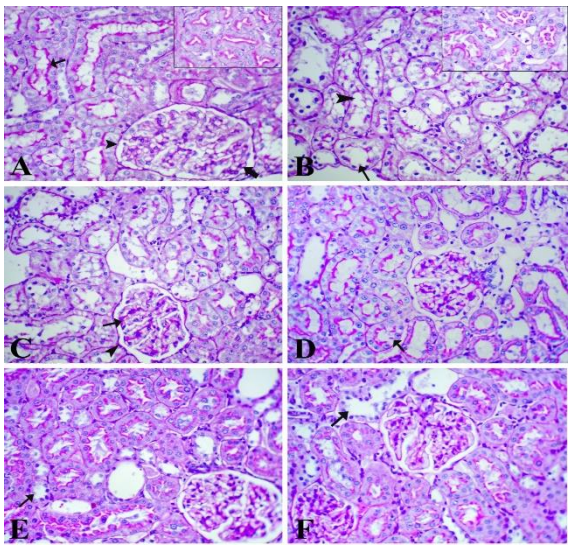

Fig.6. Photomicrographs of renal tissues stained with PAS×400. (A) Control group showing normal basement membranes of Bowman's capsule (arrowhead), glomeruli (thick arrow) and tubules (thin arrow); inset showing intact brush border structure of the proximal tubules. (B) STZ diabetic rats showing cytoplasmic vacuoles (arrowhead) with loss or fragmentation of the brush borders of proximal convoluted tubules (arrow); inset showing prominent PAS-positive material accumulation. (C) STZ diabetic rats showing mild thickened basement membranes of glomerular capillaries (arrow) and Bowman's capsule (arrowhead), (D) Glibenclamide group revealing normal PAS staining of glomeruli and tubules, with loss or fragmentation of the brush borders of a few renal tubules (arrow). (E) CSE group displaying normal PAS staining of glomeruli, with intact brush borders of nearly all proximal convoluted tubules, note loss of brush borders in a few renal tubules (arrow). (F) GE group showing normal PAS staining of glomeruli, and intact brush borders of majority of proximal convoluted tubules, and loss or fragmentation of the brush borders of a few tubules (arrow).

Heart

Cardiac sections from the control group revealed intact cardiomyocytes with centrally located nuclei and preserved myocardial blood vessels (Fig. 7A). In contrast, STZ-induced diabetic group demonstrated pronounced necrosis and myomalacia (Fig. 7B), accompanied by multifocal myocardial hemorrhage and widespread intrasarcoplasmic vacuolation within the myocardium. Furthermore, vascular damage was evident, illustrated by hypertrophy of smooth muscle (Fig. 7C), or hyalinosis and vacuolation of vascular wall (Fig. 7D).

Treatment with glibenclamide markedly mitigated the cardiac damage induced by STZ. Most examined sections exhibited histological structures closely resembling the control group (Fig. 7E). Nonetheless, a few sections showed mild pathology, including intermuscular capillary congestion and limited areas of cardiac muscle necrosis (Fig. 7F). Similarly, treatment with CSE significantly protected against STZ-induced cardiac damage. The majority of heart sections displayed normal cardiac muscle histology comparable to the control group, although minor localized necrosis was noted in some cardiac muscle fibers (Fig. 7G). Mild congestion of myocardial blood vessels and capillaries was also occasionally observed (Fig. 7H). The GE-treated group, revealed minimal cardiac alterations characterized by limited necrosis among predominantly healthy cardiac muscles (Fig. 7I). Furthermore, mild thickening of myocardial blood vessel walls and mild congestion of intermuscular capillaries were occasionally observed in a few sections (Fig. 7J).

Histopathological damage scoring

The semiquantitative scoring of pancreatic (Fig. 8), renal (Fig. 9), and cardiac (Fig. 10) tissues revealed significant damage in STZ-induced diabetic rats, characterized by β-cell necrosis (pancreas), tubular degeneration (kidneys), and myocardial necrosis (heart). Treatment with CSE and GE markedly reduced histopathological scores across all organs ($p < 0.001$ vs. diabetic group), with CSE demonstrating superior efficacy, nearly normalizing pancreatic islet architecture, preserving renal tubular integrity, and minimizing cardiac lesions. GE also demonstrated substantial protective effects, although slightly less pronounced than CSE. Glibenclamide showed intermediate protection, while untreated diabetic rats exhibited severe injury (scores >12, indicating widespread damage).

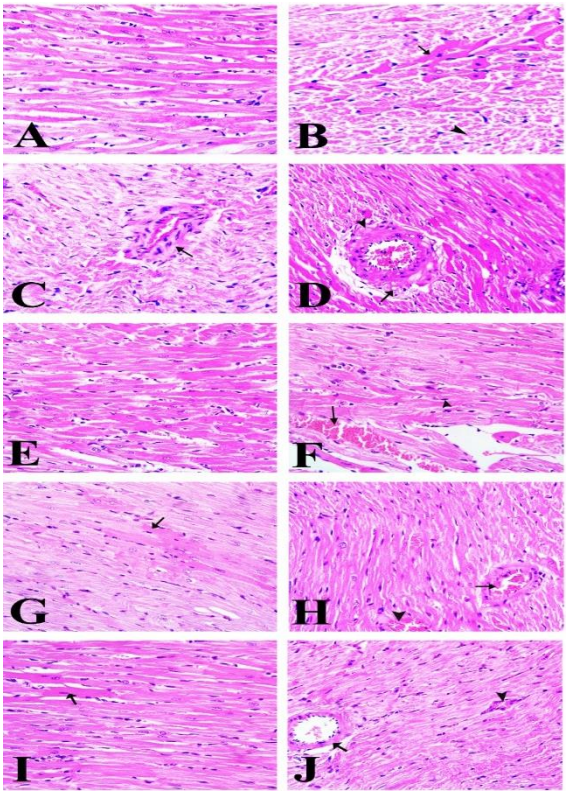

Fig.7. Representative photomicrographs of heart sections stained by H&E ×200. (A) control group revealed normal cardiomyocytes with centrally located nuclei with intact intermuscular blood capillary, (B-D) STZ diabetic group revealing (B) focal cardiac necrosis (arrow) with myomalacia (arrowhead),(C) muscular hypertrophy of blood vessel wall (arrow) with luminal narrowing, (D) hyalinosis of myocardial blood vessel (arrowhead) and vacuolation of smooth muscles of this blood vessel and some cardiac muscle (arrow), (E-F)) Diabetic rats treated with glibenclamide showing (E) cardiac muscles nearly identical to control, (F) congestion of the intermuscular capillaries(arrow) with necrosis of some cardiac muscles (arrowhead). (G-H) CSE treated group revealing (G) necrosis of a few cardiac muscles among identical cardiac muscles, (H) with mild congestion of cardiac blood vessel wall and intermuscular blood capillary (arrowhead). (I-J) GE treated group showing (I) typical intact cardiac muscles with necrosis of a few cardiac muscle (thin arrow), (J) mild thickening of cardiac blood vessel wall (arrow) and congestion of intermuscular blood capillary (arrowhead).

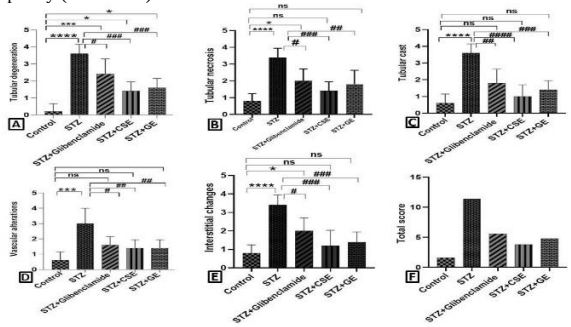

Fig.8. Semiquantitative evaluation of pancreatic histopathology and immunoreactivity. (A) Hypocellularity of the islets of Langerhans, (B) Degeneration/necrosis of islets β-cell. (C) Insulin immunoreactivity. (D) Total histopathological damage score. Data are expressed as mean ± SD. Asterisks (*) denote significance vs. control: ****$p < 0.0001$, ***$p < 0.001$, **$p < 0.01$, *$p < 0.05$; Hashtags (#) denote significance vs. STZ group: ####$p < 0.0001$, ###$p < 0.001$, #$p < 0.05$; "ns" indicates non-significant differences.

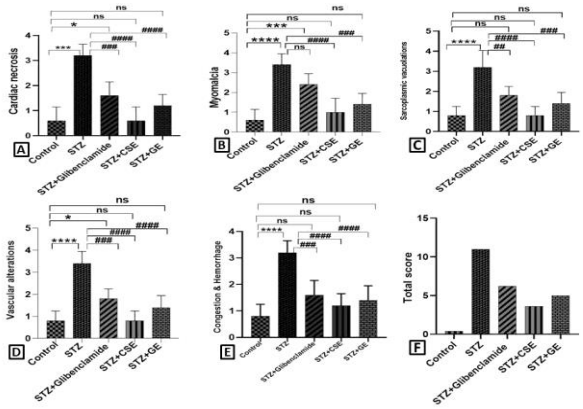

Fig.9. Semiquantitative evaluation of renal histopathology. (A)Tubular degeneration, (B) Tubular necrosis. (C) Tubular cast. (D) Vascular alteration. (E) Interstitial changes. (F) Total renal damage score. Data are expressed as mean ± SD. Asterisks (*) denote significance vs. control: ****p < 0.0001, ***p < 0.001, *p < 0.05; Hashtags (#) denote significance vs. STZ group: ####p < 0.0001, ###p <0.001, ##p < 0.01 #p < 0.05; "ns" indicates non-significant differences.

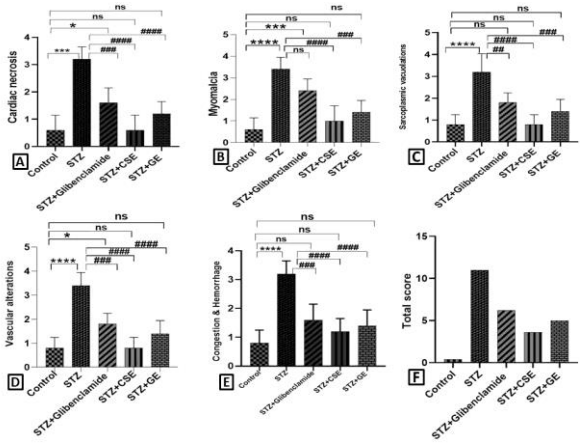

Fig.10. Semiquantitative evaluation of cardiac lesions. (A) Cardiac necrosis. (B) Myomalacia. (C) Sarcoplasmic vacuolation. (D) Vascular alteration. (E) Congestion & hemorrhage. (F) Total cardiac damage score. Data are expressed as mean ± SD. Asterisks (*) denote significance vs. control: ****p < 0.0001, ***p < 0.001, *p < 0.05; Hashtags (#) denote significance vs. STZ group ####p < 0.0001, ###p <0.001, ##p < 0.01; "ns" indicates non-significant differences.

4. DISCUSSION

Diabetes mellitus is a syndrome resulting from a variable interaction of genetic and environmental factors. It is characterized by abnormalities in insulin secretion and its receptor interaction affecting metabolism of carbohydrates, fats, and proteins cause damage to various organs (Jadon et al., 2024). Recent studies have suggested that the prevalence of pancreatic, renal, and heart dysfunctions and lesions are more frequent and severe associated with diabetes (Sarhat et al., 2019) .

Diabetic nephropathy (DN) is one of the leading causes of mortality in diabetic animals (Dagar et al., 2021). Oxidative stress is related to changes caused by continued hyperglycemia and increased advanced glycation end products (AGEs) (Samsu, 2021). Chronic changes accompanied by STZ-induced diabetes are due to the release of nitric oxide (NO), which mediates carbamoylation, alkylation of cellular components, and destruction of pancreatic β cells of Islet through DNA damage and cell necrosis (Zhu, 2022).

In the present study, STZ-induced hyperglycemia was associated with substantial pathological changes in the islets of Langerhans, including hypocellularity, degeneration, and necrosis. These changes were verified by immuno-histochemistry results, which revealed a very low immunoreactive response to anti-insulin expression. These findings were agreed with (Metawea et al., 2023). In the current investigation, daily oral administration of glibenclamide, CSE, and GE significantly lowered glucose levels and reduced pancreatic islets cell damage induced by STZ. However, the CSE and GE treatment resulted in significantly lower blood glucose levels than the glibenclamide-treated group. These findings were consistent with Moharib and Adly, (2024) and Delgado et al., (2025). The antihyperglycemic and protective effects of CSE against STZ-islet damage could be related to its polyphenol and flavonoid antioxidant substances (Mousa et al., 2021). Similarly, the antidiabetic benefits of GE were linked to the presence of allicin-type compounds or sulfur compounds [di (2-propenyl) disulfide and 2-propenyl propyl disulfide, respectively (Yan et al., 2023).

The kidney is the most important organ involved in the detoxification of advanced glycation end products (AGEs). AGEs are a complex group of modifications on proteins; they can be formed inside the body or absorbed from the diet (Twarda-Clapa et al., 2022). AGEs formation leads to structural and functional alterations of intra- and extra-cellular proteins. Furthermore, AGEs accumulation causes the induction of oxidative stress (Uceda et al., 2024). Chronic hyperglycemia and oxidative stress lead to structural abnormalities in many organs as β-cell necrosis (pancreas), tubular degeneration (kidneys), and myocardial necrosis (heart). Additionally, Functional abnormalities such as increased urea, uric acid, and creatinine levels represent the onset of DM. Oral administration of CSE and GE has reversed the increased serum renal parameters, and these attenuating effects were related to their antioxidant component. In the present study, STZ-induced hyperglycemia was associated with substantial pathological changes in renal sections, including severe degeneration and necrosis of tubular epithelium were recorded. These alterations were confirmed by periodic acid Schiff (PAS) staining. PAS is a superior stain for assessing tubule brush borders and basement membranes (Alghamdi et al., 2020)

In the current study, PAS staining revealed weakening or loss of brush borders of the proximal convoluted epithelium. On the other hand, Glibenclamide, CSE, and GE treatment reduced these changes caused by STZ-induced diabetes and preserved the renal tubules and glomeruli, which was also confirmed by PAS staining. These findings correlate with biochemical improvements, confirming the protective effects of CSE and GE for managing diabetes and its associated renal and cardiac complications. The antioxidant compounds in CSE and GE present in these extracts, might be helpful in the amelioration of chronic blood glucose levels, oxidative stress via inhibition of AGEs and their related consequences, and may be effective against the progression renal damage associated with STZ-induced diabetes (Syed et al., 2025).

Diabetes is an independent risk factor for cardiac failure (Sarhat et al., 2019). DM is associated with an increased prevalence of congestive heart failure, independent of atherosclerotic coronary artery disease (Siam et al., 2024). In this work, various cardiac microscopic alterations in the form of focal necrosis with myomalacia, intrasarcoplasmic vacuolation, as well as damage to blood vessels were noticed in the heart sections of diabetic rats. These results align with other works (Nemoto et al., 2006, Abdel-Mageid et al., 2018). These structural cardiomyocyte changes were probably due to the degeneration of the structural protein in mitochondria of the cytoplasm that occurred in diabetes (Abdel-Mageid et al., 2018). Badole et al., (2015) reported that any serious

insult to the heart muscle enhances the release of Creatine Kinase-MB (CK-MB), and Lactic Dehydrogenase (LDH) enzymes into the serum of diabetic animals. In addition, cardiac biomarkers of the STZ group, CK-MB and LDH were significantly increased. The results of the current study agreed with those of Suanarunsawat et al., (2016), who found that DM impaired cardiac functions of diabetic rats by augmenting serum levels of LDH and CK-MB. Likewise, Zhang et al., (2024) suggested that the peak rise in LDH is proportional to the extent of injury to the myocardial tissue. The current study found that oral treatment of glibenclamide, CSE, and GE considerably reduced LDH and CK-MB levels while also greatly attenuating STZ-induced myocardial injury. Due to their bioactive constituents, such as the linalool in coriander (Sharifi et al., 2023) and the allicin in garlic (Sharifi et al., 2023), CSE and GE have antioxidant properties that probably alleviate the heart damage caused by hyperglycemia-induced oxidative stress. As a result, the cardiac muscles were nearly similar to cardiac muscles in the control rats.

5. CONCLUSIONS

Both CSE and GE demonstrated greater cardiorenal protective and antidiabetic effects in a diabetic rat model. However, because of its stronger antihyperglycemic action and greater antioxidant content, CSE provided better protection overall than GE.

6. REFERENCES

1. Abdel-Mageid, A. D., Abou-Salem, M. E., Salaam, N. M. and El-Garhy, H. A. 2018. The potential effect of garlic extract and curcumin nanoparticles against complication accompanied with experimentally induced diabetes in rats. Phytomedicine, 43, 126-134.
2. Abunasef, S. K., Amin, H. A. and Abdel-Hamid, G. A. 2014. A histological and immunohistochemical study of beta cells in streptozotocin diabetic rats treated with caffeine. Folia histochemica et cytobiologica, 52, 42-50.
3. Ahmed, G. M., Abdelaziz, H. O., El Sayed, H. M. and Adly, M. A. 2023. Histopathological Changes on The Kidney and Lung of Experimentally Induced Diabetic Rats. SVU-International Journal of Medical Sciences, 6, 594-601.
4. Alghamdi, M. A., Hussein, A. M., Al-Eitan, L. N., Elnashar, E., Elgendy, A., Abdalla, A. M., Ahmed, S. and Khalil, W. A. 2020. Possible mechanisms for the renoprotective effects of date palm fruits and seeds extracts against renal ischemia/reperfusion injury in rats. Biomedicine & Pharmacotherapy, 130, 110540. https://doi.org/10.1016/j.biopha.2020.110540
5. Aloke, C., Egwu, C. O., Aja, P. M., Obasi, N. A., Chukwu, J., Akumadu, B. O., Ogbu, P. N. and Achilonu, I. 2022. Current advances in the management of diabetes mellitus. Biomedicines, 10, 2436.
6. Babel, R. A. and Dandekar, M. P. 2021. A review on cellular and molecular mechanisms linked to the development of diabetes complications. Current Diabetes Reviews, 17, 457-473.
7. Badole, S. L., Chaudhari, S. M., Jangam, G. B., Kandhare, A. D. and Bodhankar, S. L. 2015. Cardioprotective Activity of Pongamia pinnata in Streptozotocin-Nicotinamide Induced Diabetic Rats. BioMed research international, 2015, 403291. https://doi.org/10.1155/2015/403291
8. Bancroft, J. D. and Layton , C. 2019. The hematoxylin and eosin. In: Suvarna, S.K., Layton, C., Bancroft, J.D. (Eds.), . Bancroft's Theory and Practice of Histological Techniques, 8th Ed. Elsevier, Philadelphia, , pp. 126–138 .
9. Chavez, R., Fraser, D. J., Bowen, T., Jenkins, R. H., Nesargikar, P., Pino-Chavez, G. and Khalid, U. 2016. Kidney ischaemia reperfusion injury in the rat: the EGTI scoring system as a valid and reliable tool for histological assessment. Journal of Histology and Histopathology, 3. http://dx.doi.org/10.7243/2055-091X-3-1
10. Dagar, N., Das, P., Bisht, P., Taraphdar, A. K., Velayutham, R. and Arumugam, S. 2021. Diabetic nephropathy: A twisted thread to unravel. Life sciences, 278, 119635.
11. Delgado, E. M. M., Quiroz-Aldave, J. E., del Carmen Durand-Vásquez, M., Aldave-Pita, L. N., Fuentes-Mendoza, J. M., Concepción-Urteaga, L. A., Paz-Ibarra, J. and Concepción-Zavaleta, M. J. 2025. Immunomodulatory effect of allium sativum in type 2 diabetes mellitus. World Journal of Experimental Medicine, 15, 103481.
12. Dunn, S. R., Qi, Z., Bottinger, E. P., Breyer, M. D. and Sharma, K. 2004. Utility of endogenous creatinine clearance as a measure of renal function in mice. Kidney international, 65, 1959-1967.
13. Eidi, A., Eidi, M. and Esmaeili, E. 2006. Antidiabetic effect of garlic (Allium sativum L.) in normal and streptozotocin-induced diabetic rats. Phytomedicine, 13, 624-629.
14. El-Shaer, N. O., Hegazy, A. M. and Muhammad, M. H. 2023. Protective effect of quercetin on pulmonary dysfunction in streptozotocin-induced diabetic rats via inhibition of NLRP3 signaling pathway. Environmental Science and Pollution Research, 30, 42390-42398.
15. Ghanbari, E., Nejati, V. and Khazaei, M. 2016. Improvement in serum biochemical alterations and oxidative stress of liver and pancreas following use of royal jelly in streptozotocin-induced diabetic rats. Cell Journal (Yakhteh), 18, 362. https://doi.org/10.22074/cellj.2016.4564
16. Jadon, A. S., Kaushik, M. P., Anitha, K., Bhatt, S., Bhadauriya, P. and Sharma, M. 2024. Types of diabetes mellitus, mechanism of insulin resistance and associated complications. Biochemical immunology of diabetes and associated complications. Elsevier. https://doi.org/10.1016/B978-0-443-13195-0.00001-6
17. Jing, W., Jabbari, B. and Vaziri, N. D. 2018. Uremia induces upregulation of cerebral tissue oxidative/inflammatory cascade, down-regulation of Nrf2 pathway and disruption of blood brain barrier. American journal of translational research, 10, 2137-2147.
18. Kaur, G., Padiya, R., Adela, R., Putcha, U. K., Reddy, G., Reddy, B., Kumar, K., Chakravarty, S. and Banerjee, S. K. 2016. Garlic and resveratrol attenuate diabetic complications, loss of β-cells, pancreatic and hepatic oxidative stress in streptozotocin-induced diabetic rats. Frontiers in Pharmacology, 7, 360. Doi: 10.3389/fphar.2016.00360
19. Layton, C. and Bancroft, J. D. 2019. Carbohydrates . In: Suvarna, S.K., Layton, C., Bancroft, J.D. (Eds.), Bancroft's Theory and Practice of Histological Techniques, 8th Ed. . Elsevier, Philadelphia, pp. 176–187.
20. Lidiková, J., Čeryová, N., Tóth, T., Musilová, J., Vollmannová, A., Mammadova, K. and Ivanišová, E. 2022. Garlic (Allium sativum L.): characterization of bioactive compounds and related health benefits. Herbs and Spices-New Advances. IntechOpen. DOI: 10.5772/intechopen.108844
21. Metawea, M. R., Abdelrazek, H. M., El-Hak, H. N. G., Moghazee, M. M. and Marie, O. M. 2023. Comparative effects of curcumin versus nano-curcumin on histological, immunohistochemical expression, histomorphometric, and biochemical changes to pancreatic beta cells and lipid profile of streptozocin induced diabetes in male Sprague–Dawley rats. Environmental Science and Pollution Research, 30, 62067-62079.
22. Mittal, P. and Juyal, V. 2012. Drug-dietary interaction potential of garlic on glimepiride treated type 2 diabetic Wistar rats. Journal of Diabetology, 3, 3 DOI:10.4103/2078-7685.
23. Moharib, S. A. and Adly, R. S. 2024. Hypoglycemic and hepatoprotective activities of coriander (Coriandrum sativum) Extract in Streptozocin Induced Diabetic Rats. Journal of Advances in Biology & Biotechnology, 27, 15-38.
24. Mousa, A. M., Soliman, K. E., Alhumaydhi, F., Almatroudi, A., Al Rugaie, O., Allemailem, K. S., Alrumaihi, F., Khan, A., Rezk, M. Y. and Aljasir, M. 2021. Garlic Extract Alleviates Trastuzumab-Induced Hepatotoxicity in Rats Through Its Antioxidant, Anti-Inflammatory, and Antihyperlipidemic Effects. Journal of Inflammation Research, 6305-6316.
25. Nambirajan, G., Karunanidhi, K., Ganesan, A., Rajendran, R., Kandasamy, R., Elangovan, A. and Thilagar, S. 2018. Evaluation of antidiabetic activity of bud and flower of Avaram Senna (Cassia auriculata L.) In high fat diet and streptozotocin induced diabetic rats. Biomedicine & Pharmacotherapy, 108, 1495-1506.

26. Naquvi, K. J., Ali, M. and Ahmad, J. 2004. Antidiabetic activity of aqueous extract of Coriandrum sativum L. fruits in streptozotocin induced rats. Indian J Exp Biol, 42, 909-12.
27. Nemoto, O., Kawaguchi, M., Yaoita, H., Miyake, K., Maehara, K. and Maruyama, Y. 2006. Left ventricular dysfunction and remodeling in streptozotocin-induced diabetic rats. Circulation Journal, 70, 327-334.
28. Okoro, B. C., Dokunmu, T. M., Okafor, E., Sokoya, I. A., Israel, E. N., Olusegun, D. O., Bella-Omunagbe, M., Ebubechi, U. M., Ugbogu, E. A. and Iweala, E. E. J. 2023. The ethnobotanical, bioactive compounds, pharmacological activities and toxicological evaluation of garlic (Allium sativum): A review. Pharmacological Research-Modern Chinese Medicine, 8, 100273. https://doi.org/10.1016/j.prmcm.2023.100273
29. Padiya, R., Khatua, T. N., Bagul, P. K., Kuncha, M. and Banerjee, S. K. 2011. Garlic improves insulin sensitivity and associated metabolic syndromes in fructose fed rats. Nutrition & metabolism, 8, 1-8.
30. Priya, A. V. and Kumar, V. S. 2021. A Comprehensive Review OnCoriandrumSativum Linn. NeuroQuantology, 19, 148. DOI: 10.14704/nq.2021.19.6.NQ21080
31. Rabbani, S. I., Devi, K. and Khanam, S. 2010. Protective role of glibenclamide against nicotinamidestreptozotocin induced nuclear damage in diabetic Wistar rats. Journal of Pharmacology and Pharmacotherapeutics, 1, 18-23.
32. Rashid, H., Jali, A., Akhter, M. S. and Abdi, S. A. H. 2023. Molecular mechanisms of oxidative stress in acute kidney injury: Targeting the loci by resveratrol. International Journal of Molecular Sciences, 25, 3. https://doi.org/10.3390/ijms25010003.
33. Sadeghabadi, Z. A., Lotfi, F., Moheb, S. S., Abbasalipourkabir, R., Goodarzi, M. T. and Ziamajidi, N. 2022. Effects of garlic extract on inflammatory cytokines in rats with type 1 and type 2 diabetes. Gene Reports, 26, 101474. https://doi.org/10.1016/j.genrep.2021.101474
34. Samsu, N. 2021. Diabetic nephropathy: challenges in pathogenesis, diagnosis, and treatment. BioMed research international, 2021, 1497449. https://doi.org/10.1155/2021/1497449
35. Sarhat, E., Wadi, S., Sedeeq, B., Sarhat, T. R. and Jasim, N. 2019. Study of histopathological and biochemical effect of Punica granatum L. extract on streptozotocin-induced diabetes in rabbits. Iraqi Journal of Veterinary Sciences, 33, 189-194.
36. Saunders, H., Loong, D., Mishra, S., Ashoor, H. M., Antony, J., Darvesh, N., Bains, S. K., Jamieson, M., Plett, D. and Trivedi, S. 2022. The cost-effectiveness of intermediate-acting, long-acting, ultralong-acting, and biosimilar insulins for type 1 diabetes mellitus: a systematic review. Value in Health, 25, 1235-1252.
37. Shabab, S., Mahmoudabady, M., Gholamnezhad, Z., Fouladi, M. and Asghari, A. A. 2024. Diabetic cardiomyopathy in rats was attenuated by endurance exercise through the inhibition of inflammation and apoptosis. Heliyon, 10. https://doi.org/10.1016/j.heliyon.2023.e23427
38. Siam, N. H., Snigdha, N. N., Tabasumma, N. and Parvin, I. 2024. Diabetes Mellitus and Cardiovascular Disease: exploring epidemiology, pathophysiology, and treatment strategies. Reviews in Cardiovascular Medicine, 25, 436.
39. Sobhani, Z., Mohtashami, L., Amiri, M. S., Ramezani, M., Emami, S. A. and Simal-Gandara, J. 2022. Ethnobotanical and phytochemical aspects of the edible herb Coriandrum sativum L. Journal of Food Science, 87, 1386-1422.
40. Song, B., Shu, Y., Cui, T. and Fu, P. 2015. Allicin inhibits human renal clear cell carcinoma progression via suppressing HIF pathway. International Journal Of Clinical And Experimental Medicine, 8, 20573-20580.
41. Soni, B., Visavadiya, N. P. and Madamwar, D. 2009. Attenuation of diabetic complications by C-phycoerythrin in rats: antioxidant activity of C-phycoerythrin including copper-induced lipoprotein and serum oxidation. British Journal of Nutrition, 102, 102-109.
42. Suanarunsawat, T., Anantasomboon, G. and Piewbang, C. 2016. Anti-diabetic and anti-oxidative activity of fixed oil extracted from Ocimum sanctum L. leaves in diabetic rats. Experimental and therapeutic medicine, 11, 832-840.
43. Syed, R. U., Moni, S. S., Hussein, W., Alhaidan, T. M. S., Abumilha, S. M. Y., Alnahdi, L. K., Wong, L. S., Subramaniyan, V. and Kumarasamy, V. 2025. Effect of cubebin against streptozotocin-induced diabetic nephropathy rats via inhibition TNF-α/NF-κB/TGF-β: in vivo and in silico study. Scientific Reports, 15, 4369. https://doi.org/10.1038/s41598-025-87319-7
44. Tan, Y., Zhang, Z., Zheng, C., Wintergerst, K. A., Keller, B. B. and Cai, L. 2020. Mechanisms of diabetic cardiomyopathy and potential therapeutic strategies: preclinical and clinical evidence. Nature Reviews Cardiology, 17, 585-607.
45. Thijs, L., Asayama, K., Maestre, G. E., Hansen, T. W., Buyse, L., Wei, D.-M., Melgarejo, J. D., Brguljan-Hitij, J., Cheng, H.-M. and de Souza, F. 2021. Urinary proteomics combined with home blood pressure telemonitoring for health care reform trial: rational and protocol. Blood pressure, 30, 269-281.
46. Tiffany, T., Jansen, J., Burtis, C., Overton, J. and Scott, C. 1972. Enzymatic kinetic rate and end-point analyses of substrate, by use of a GeMSAEC fast analyzer. Clinical Chemistry, 18, 829-840.
47. Tong, X., Yu, Q., Ankawi, G., Pang, B., Yang, B. and Yang, H. 2020. Insights into the role of renal biopsy in patients with T2DM: a literature review of global renal biopsy results. Diabetes Therapy, 11, 1983-1999.
48. Twarda-Clapa, A., Olczak, A., Białkowska, A. M. and Koziołkiewicz, M. 2022. Advanced glycation end-products (AGEs): Formation, chemistry, classification, receptors, and diseases related to AGEs. Cells, 11, 1312.
49. Uceda, A. B., Mariño, L., Casasnovas, R. and Adrover, M. 2024. An overview on glycation: molecular mechanisms, impact on proteins, pathogenesis, and inhibition. Biophysical Reviews, 16, 189-218.
50. Wang, N. and Zhang, C. 2024. Oxidative Stress: A Culprit in the Progression of Diabetic Kidney Disease. Antioxidants, 13, 455. https://doi.org/10.3390/antiox13040455
51. Wild, S., Roglic, G., Green, A., Sicree, R. and King, H. 2004. Global prevalence of diabetes: estimates for the year 2000 and projections for 2030. Diabetes care, 27, 1047-1053.
52. Yan, J.-K., Zhu, J., Liu, Y., Chen, X., Wang, W., Zhang, H. and Li, L. 2023. Recent advances in research on Allium plants: Functional ingredients, physiological activities, and applications in agricultural and food sciences. Critical Reviews in Food Science and Nutrition, 63, 8107-8135.
53. Young, D. S. 1995. Effects of drugs on clinical laboratory tests. Annals Clinical Biochemistry, 34: 579-581. https://doi.org/10.1177/000456329703400601
54. Zhang, H., Kang, K., Chen, S., Su, Q., Zhang, W., Zeng, L., Lin, X., Peng, F., Lin, J. and Chai, D. 2024. High serum lactate dehydrogenase as a predictor of cardiac insufficiency at follow-up in elderly patients with acute myocardial infarction. Archives of Gerontology and Geriatrics, 117, 105253. https://doi.org/10.1016/j.archger.2023.105253
55. Zhu, B. T. 2022. Pathogenic mechanism of autoimmune diabetes mellitus in humans: potential role of streptozotocin-induced selective autoimmunity against human islet β-cells. Cells, 11, 492. https://doi.org/10.3390/cells11030492.